Polymer 49 (2008) 4271–4278

Contents lists available at ScienceDirect

Polymer

journal homepage: www.elsevier.com/locate/polymer

Crystallization of oriented isotactic polypropylene (iPP) in the presence of in situ poly(ethylene terephthalate) (PET) microfibrils

Gan-Ji Zhong [a], Zhong-Ming Li [a,*], Liangbin Li [b], Kaizhi Shen [a]

[a] College of Polymer Science and Engineering, State Key Laboratory of Polymer Materials Engineering, Sichuan University, Chengdu, Sichuan 610065, PR China
[b] National Synchrotron Radiation Laboratory, Department of Polymer Science and Engineering, University of Science and Technology of China, Hefei 230026, PR China

ARTICLE INFO

Article history:
Received 2 January 2008
Received in revised form 24 April 2008
Accepted 28 July 2008
Available online 3 August 2008

Keywords:
Oriented iPP melt
PET microfibrils
Oriented crystalline morphology

ABSTRACT

The present article reports the nonisothermal crystallization process and morphological evolution of oriented iPP melt with and without in situ poly(ethylene terephthalate) (PET) microfibrils. The bars of neat iPP and PET/iPP microfibrillar blend were fabricated by shear controlled orientation injection molding (SCORIM), which exhibit the oriented crystalline structure (shish–kebab), especially in the skin layer. The skin layer was annealed at just above its melting temperature (175 °C) for a relatively short duration (5 min) to preserve a certain level of oriented iPP molecules. It was found that the existence of ordered clusters (i.e. oriented iPP molecular aggregates) leads to the primary nucleation at higher onset crystallization temperature, and formation of the fibril-like crystalline morphology. However, the overall crystallization rate decreases as a result that the relatively high crystallization temperature restrains the secondary nucleation. With the existence of PET microfibrils, the heterogeneous nucleation distinctly occurs in the unoriented iPP melt and results in the increase of crystallization peak temperature and overall crystallization rate, for the first time, we observed that the onset crystallization temperature has been enhanced further with addition of PET microfibrils in the oriented iPP melt, indicating the synergistic effect of row nucleation and heterogeneous nucleation under quiescent condition.

1. Introduction

Nowadays, the fiber reinforced semi-crystalline polymer composites have been widely used, and injection molding is one of the most important methods for their fabrication. It is well known that the oriented crystallization, rather than quiescent crystallization, always occurs during injection molding, and the structure formed, such as skin–core structure [1–7], shish–kebab structure [7,8], will affect the final properties of parts distinctly. The oriented crystallization in the presence of fibers has been reported by a few researchers [9–11], Marom and coworkers have investigated the oriented crystallization of iPP containing ultrahigh molecular weight PE (UHMWPE) fiber [9] and aramid fiber (AF) [10], they found that the presence of oriented UHMWPE fibers or AF significantly facilitated the crystallization of iPP and enhanced the initial shish–kebab structure, and argued that shear flow orients the fibers, and the interfacial friction between fibers and matrix effectively retards the relaxation of iPP chains, their recent results clearly indicated that the effect is synergistic rather than additive [11]. However, in these investigations, a shearing hot stage was usually utilized to shear a melt for investigation of oriented crystallization, it is known that the flow field (or profile) during injection molding, such as "fountain" flow [12], is more complex than that in shear cell, therefore, a strategy being closer in practice to injection molding should be utilized to study the oriented crystallization of fiber reinforced polymer composites.

The in situ characterization for oriented crystallization during injection molding is undoubtedly an effective and direct approach to reveal crystalline morphology evolution; however, it faces many practical challenges. Fortunately, some ordered structures with long-lived stability, induced by flow, appear to persist in the melt far above the nominal melting point [13], which can serve as nucleation sites for subsequent re-crystallization. Recently, these ordered structures, also called flow induced crystal nucleation precursors, attracted the attention of several research groups [14–19]. Kornfield and coworkers discovered that the "shear-induced structures" formed at a temperature of 175 °C in the sheared iPP melt [14,15]. Alfonso et al. investigated the relaxation process of shear induced nucleation precursors in a temperature range above melting point, and it is found that the relax of high molecular weight samples is slower than that sample with short chains and can keep the memory of shear induced structuring during several hours [16]. Hsiao and coworkers probed the nature of the structures (prior to crystallization) induced by flow, the

* Corresponding author. Tel./fax: +86 28 8540 5324.
E-mail address: zm_li@263.net.cn (Z.-M. Li).

0032-3861/$ – see front matter © 2008 Elsevier Ltd. All rights reserved.
doi:10.1016/j.polymer.2008.07.056

results suggested that oriented structures or aggregates formed and remained stable for a long time (up to 2 h after shear) at 175 °C [17], their further investigations showed that the long chains are primarily responsible for the formation of the crystallization precursor structure (especially shish) under flow [18]. However, recently, Kornfield et al. reported that the longest chains just play a catalytic role, recruiting other chains adjacent to them into formation of the shish [19]. Although the exact nature of crystal precursor is currently under investigation, the experimental results clearly suggest that the shear induced crystal precursor can preserve their orientation to some extend at relatively low annealing temperature and for a certain time, and the shish–kebab structure can form once again from the re-crystallization of oriented iPP melt [20], thus reflecting the evolution of crystalline morphology during practical semi-crystalline polymer processing. That is to say, the investigation on the morphology evolution of re-crystallization for a semi-crystalline polymer with flow induced crystal precursors can reflect the crystallization of practical polymer processing more directly than that using the shearing hot stage as long as the annealing temperature and the duration time are proper.

In our previous work, the so-called microfibrillar blends based on thermoplastic engineering polymers (TEP) and polyolefins (PO) mainly polyethylene and polypropylene have been prepared through a "slit die extrusion-hot stretch-quenching" process, aiming at developing a simple and convenient approach to property enhancement of commodity polymers and recycling of thermoplastic polymer waste [21,22]. It was found that the in situ poly(ethylene terephthalate) (PET) microfibrils can act as an effective nucleating agent for iPP and PE [23,24], three origins for crystal nucleation under shear flow field exist: (a) the classical row nucleation, (b) fibril nuclei and (c) nuclei induced by fibril assistant alignment [25]. In the later work, the injection molded bars of the PET/iPP microfibrillar blends were prepared by conventional injection molding (CIM) and by shear controlled orientation injection molding (SCORIM). Note that the feature of SCORIM is that the vibrational shear stress can impose on polymer melt during packing stage, hence leading to a high level of molecular orientation even in the core region [26,27], which is a good tool to investigate the effect of complex flow field during the practical polymer processing on the morphology as well as properties of semi-crystalline polymers and their blends. It was observed that the molecules in whole region (especially in skin layer) of SCORIM bars are oriented greatly to the molding direction and shish–kebab structure can form [28], and the existence of three-dimensional PET microfibrillar network in iPP melt during SCORIM process, refining the flow field and accelerating nucleation of iPP, led to the bars with homogeneous orientation distribution across the thickness direction [29].

In this study, the aim is to probe further the evolution of crystalline morphology during the SCORIM. The skin layer and core layer were separated from the SCORIM or CIM injection molded bars of neat iPP and PET/iPP microfibrillar blend. The samples with memory of flow induced nucleation precursor were obtained through annealing at a proper annealing temperature for a short duration time, and then the crystallization of the oriented iPP melt in the presence of PET microfibrils was performed. Differential scanning calorimeter (DSC) and polarized optical microscope (POM) were used to illustrate the crystalline morphology evolution of PET/iPP microfibrillar blend during SCORIM.

2. Experimental

2.1. Materials

The materials used in this study are PET and iPP. The PET as the microfibrillar candidate is a commercial grade of textile polyester and was supplied in pellets by LuoYang Petroleum Chemical Co. (China) with $\overline{M}_n$ of ca. 2.3×10^4 g/mol. Its melting point by DSC is ca. 255 °C. The iPP used as the matrix is Model F401, a commercial product of Lanzhou Petroleum Chemical Co. (China) with $\overline{M}_n$ of ca. 11.0×10^4 g/mol and its melt flow index (MFI) is 2.5 g/10 min (190 °C, 21.6 N). In order to avoid hydrolysis, the PET was dried in a vacuum oven at 100 °C for at least 12 h prior to processing.

2.2. Preparation of PET/iPP microfibrillar blend

The PET/iPP microfibrillar blend was prepared through the "extrusion-hot stretch-quenching" process under the processing temperature of PET (ca. 270 °C) [21]. The extrusion of the PET and iPP mixture (15/85 by weight) was performed on a single-screw extruder having a screw length to screw diameter, L/D, of 30. The die for the extruder is a slit die with 35 mm width and 1.0 mm thickness. The temperature profile from the hopper to the die was 190, 250, 275, and 270 °C, respectively, and the screw rotation was maintained at 65 rpm. The extrudate was hot stretched by a take-up device with two pinching rolls to form the microfibrils. The roll temperature was kept at about 40 °C, through adjusting the volume flow rate of tap water in them. Different hot stretch ratios (HSRs, the ratio of the area of the transverse section of the die to the area of the transverse section of the extrudate) could be obtained by changing the speed of the take-up device. In this study, the HSR was set as 2.0. The PET microfibrils are ca. 1–10 μm in diameter as observed in our previous work [28]. For comparison purposes, the neat iPP has also undergone the same "extrusion-hot stretch-quenching" process.

2.3. Processing of PET/iPP microfibrillar blend bar by SCORIM

The extrudate was pelletized, and then dried for 8 h at 80 °C. The dried pellets were injected into a mold in an injection molding machine at 200 °C with an injection pressure of 90 MPa. Then, SCORIM technology was applied with a frequency of 0.3 Hz and a pressure of 6 MPa for fabrication of SCORIM bars of neat iPP and PET/iPP microfibrillar blend. The mold temperature was about 40 °C. The feature of a melt flow pattern during SCORIM is quite different from that of the conventional injection molding (CIM) [26,27,30], and the remarkable difference between the two technologies exists in packing stage, whereas the other stages (i.e. preplasticizing, injection, etc.) are unchanged. During the packing stage of SCORIM, the two pistons move out of phase and the shear force would make the iPP melt move reciprocatively in the length direction of bars, and the shear flow of iPP melt takes place until the gate is solidified. In other words, before being frozen, the iPP melt continuously undergoes repeated shear stress, unless the pistons are stopped. As a result of this, the high shear stress can impose on the melt in interior region with increasing the thickness of solidified layer. The CIM was also carried out under static packing (no vibration) under the same processing temperatures. Note that, the processing temperature in this stage is far below the melting point of PET (around 255 °C), therefore, the PET microfibrils can be well preserved in bars [31].

2.4. DSC characterization

The type of DSC is Netzsch DSC 204. For preparing the samples for the DSC measurement, the skin layer and the core layer had been cut away from the injection molded bars of neat iPP and PET/iPP microfibrillar blend. The skin layer is defined as a layer with the depth from surface to 0.5 mm away from surface, and the core layer is about 1.5 mm down from the surface of the bars.

To investigate the melting behavior, the samples were heated to 200 °C with the heating rate of 10 °C/min. To characterize the

crystallization process, the detailed procedure is as follows: (a) the sample (5–10 mg) was heated to 175 °C with a heating rate of 30 °C/min; (b) kept at this temperature for 5 min; (c) cooled the sample down to 50 °C with the cooling rate of 10 °C/min; (d) for comparison, the same samples were heated again to 200 °C and held it for 5 min in order to erase the melt memory and then the step (c) was repeated.

2.5. POM observation

The crystalline morphology evolution of neat iPP sample as well as that with the presence of PET microfibrils was observed by a Leica DMIP polarized optical microscope (POM) equipped with a Linkam THMS 600 hot stage. A thin slice from skin layer (i.e. the location less than 0.5 mm away from surface) of SCORIM bar of neat iPP was melt and squeezed between two microscopic glasses at 175 °C for 5 min, and then, samples were cooled to room temperature at 2 °C/min for morphology observation. The same samples were also heated to 200 °C and held it for 5 min in order to erase the orientation memory and then cooled to room temperature at 2 °C/min for morphology observation.

For the observation of iPP crystallization with the presence of PET microfibrils, the matrix iPP in PET/iPP microfibrillar blend was etched away clearly by hot xylene (ca. 120 °C) and the PET microfibrils remained can be introduced into the neat iPP sample. And then, the same procedure mentioned in above paragraph was carried out.

3. Results and discussion

3.1. The melting behavior of different layers in SCORIM bars

The melting behavior of skin and core layers in the CIM and SCORIM bars of neat iPP is shown in Fig. 1. As shown in Table 1, one can see that the melting peaks (T_p) of the skin layers (ca. 169 and 171 °C) are always higher than that of the core layer (ca. 166 and 167 °C) for both CIM and SCORIM bars. Furthermore, the temperatures at which endotherms end (T_{end}) are different between two layers, the skin layers (ca. 178 and 176 °C) have higher T_{end} than the core layers (ca. 172 and 174 °C), indicating that the formation of oriented crystalline structure (i.e. shish–kebab structure) results in the higher melting temperature and T_{end} [32]. The similar tendency

Table 1
The melting point (T_p) and the end of melting temperature (T_{end}) in the different layers of CIM samples and SCORIM samples

Samples	Neat iPP		PET/iPP microfibrillar blend	
	T_p (°C)	T_{end} (°C)	T_p (°C)	T_{end} (°C)
Skin layer of CIM sample	169	178	165	175
Core layer of CIM sample	166	172	165	171
Skin layer of SCORIM sample	171	176	166	174
Core layer of SCORIM sample	167	174	165	175

is observed in the CIM bar of PET/iPP microfibrillar blend (see Fig. 2 and Table 1), where T_{end} is ca. 175 °C in the skin layer but 171 °C in the core layer. However, the T_p almost kept unchanged, which may ascribe to increased unperfection of crystals. The heterogeneous nucleation of PET microfibrils accelerates the crystallization and increases the unperfection of crystals.

Interestingly, unlike the neat iPP bars, the two layers in SCORIM bar of PET/iPP microfibrillar blend almost have the same T_p and T_{end} (see Fig. 2c and d and Table 1). This is quite possibly due to the more uniform distribution of crystalline structure as a result of addition of PET microfibrillar network [29]. In other words, micro-channels or pores were formed by the microfibrillar network, which acted as stir to define and homogenize the flow field in iPP melt across the thickness direction; on the other hand, the effective nucleation effect of PET microfibrils enhanced iPP crystallization. Both these two factors contributed to the homogeneous crystalline structure across the thickness direction. Although it is well known that the melting temperature of shish is several degrees higher than that of kebabs, we do not observe an additional small peak in the DSC curves, quite possibly, the fraction of shish is too low to produce the seeable endothermic peaks.

The above results reveal that the oriented crystalline structure (shish–kebab) exists in the skin layer of the SCORIM bars. Usually, the oriented aggregates in oriented crystals can survive nearly above melting temperature for a long period time [13–17]. It has been well established that it will determinedly take some time for the oriented iPP molecules to relax into random state after melted. This feature offers us an opportunity to investigate how the iPP melt with different degree of molecule orientation crystallizes, through altering the annealing temperature and duration time of the oriented iPP samples.

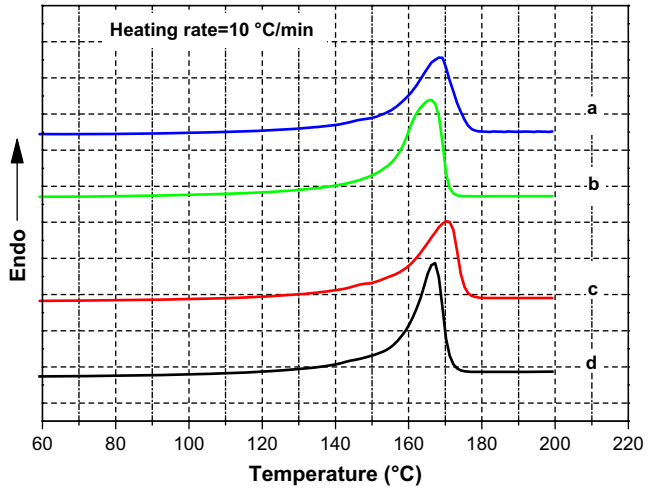

Fig. 1. DSC scans of different layers in CIM sample of neat iPP and its SCORIM sample: (a) the skin layer of CIM sample; (b) the core layer of CIM sample; (c) the skin layer of SCORIM sample; (d) the core layer of SCORIM sample.

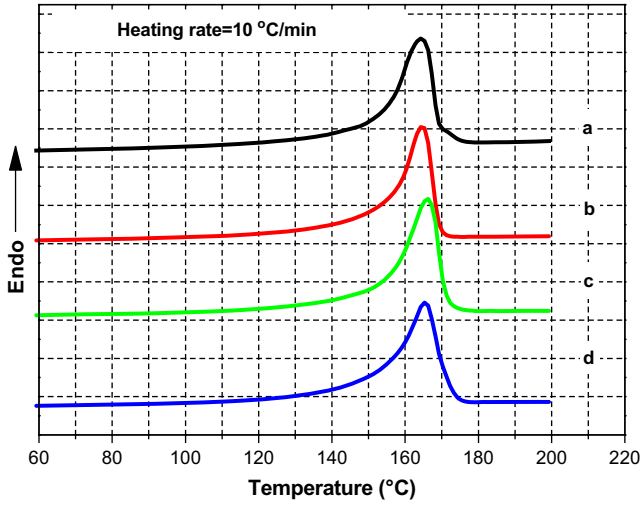

Fig. 2. DSC scans of different layers in CIM sample of PET/iPP microfibrillar blend and its SCORIM sample: (a) the skin layer of CIM sample; (b) the core layer of CIM sample; (c) the skin layer of SCORIM sample; (d) the core layer of SCORIM sample.

3.2. Nonisothermal crystallization of oriented iPP melts

In order to investigate the crystallization of oriented iPP melt, the skin layers were cut from the SCORIM bars of both neat iPP and PET/iPP microfibrillar blend (see Section 2 for details), and then examined by DSC. The nonisothermal crystallization curves with different annealing temperatures and annealing time are shown in Fig. 3. The relative crystallinity, $X(T)$, is calculated by [23]

$$X(T) = \frac{\int_{T_0}^{T}\left(\frac{dH}{dt}\right)dt}{\int_{T_0}^{T_2}\left(\frac{dH}{dt}\right)dt} \times 100\% \quad (1)$$

where T_0 and T_2 are the onset and end of crystallization temperatures, respectively, and dH/dt is the heat-evolution rate. Fig. 4 shows the relative crystallinity, $X(T)$, as a function of temperature at a cooling rate of 10 °C/min.

As illustrated in Figs. 3 and 4, for the neat iPP sample, when the sample is annealed at 175 °C for 5 min, the onset crystallization temperature is ca. 129 °C whereas it reduces to ca. 121 °C at 200 °C for 5 min, however, the maximum crystallization temperature does not change with the annealing temperatures. It is interesting that, for the sample annealed at 175 °C for 5 min, there is an additional small crystallization peak at higher temperature (ca. 124 °C), which

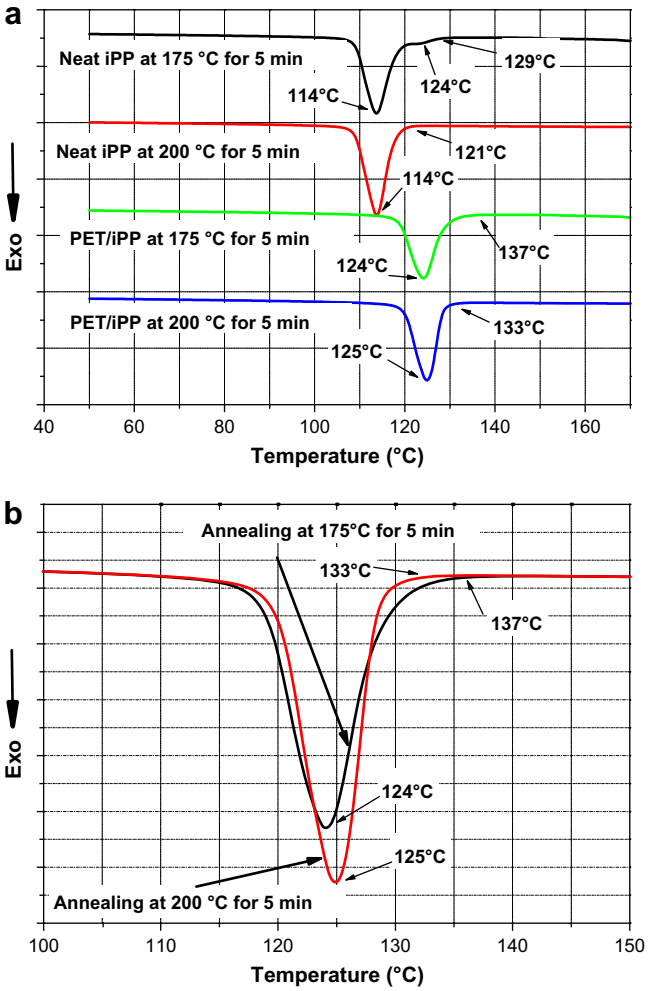

Fig. 3. Nonisothermal crystallization of neat iPP and PET/iPP microfibrillar blend with different annealing temperatures and annealing time. (a) The cooling rate is 10 °C/min, the sample cut from the skin layer of the SCORIM bars of both neat iPP parts and PET/iPP microfibrillar blend parts and (b) is the local enlargement for the sample of PET/iPP microfibrillar blend.

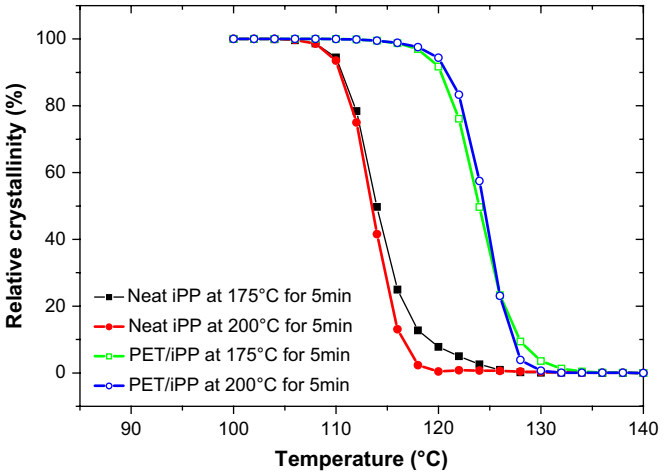

Fig. 4. Plots of relative crystallinity ($X(T)$) vs. temperature for neat iPP and PET/iPP microfibrillar blend with different annealing temperatures and annealing time at a predetermined cooling rate of 10 °C/min.

is attributed to self-seed crystallization of ordered clusters surviving in melt. And the unchanged maximum crystallization temperature reflects that the crystallization of oriented iPP melt includes two kinds of crystallization processes, i.e. the ordered cluster induced crystallization (most possible crystallization of shish–kebab) and the common point-like nuclei induced crystallization.

For the PET/iPP microfibrillar blend, when the sample is annealed at 200 °C for 5 min, the crystallization curve is quite different from the neat iPP, the onset and peak crystallization temperatures for PET/iPP microfibrillar blend are distinctly higher than the counterparts (i.e. around 133 and 125 °C, respectively, see Fig. 3), due to the heterogeneous nucleation of PET microfibrils [23,24,33]. The PET microfibrils act as heterogeneous nuclei, resulting in the increased onset and maximum crystallization temperatures. When the microfibrillar sample was annealed at 175 °C for 5 min (see Figs. 3b and 4), the onset of crystallization temperature increases further to ca. 137 °C, indicating that the synergistic effect of PET microfibrils on the iPP crystallization exists in the oriented iPP melt in the presence of PET microfibrils. In our previous works, it is found that the transcrystallization occurs in PET/iPP microfibrillar blend under quiescent condition [23,24], suggesting the existence of the relatively strong interaction between the surface of PET microfibrils and iPP molecules in vicinity of PET microfibrils, since it is reported that the high surface energy would be in favor of transcrystalline growth [34]. Therefore, we argued that the interaction may suppress the relaxation of shear induced nucleation precursors, and the larger oriented entities can survive and increase the onset of crystallization temperature. However, the direct evidence is lacked for clarifying the arguments. The further mechanism should be investigated on this synergistic effect for nucleation observed for the first time under quiescent condition.

Using $t = (T_0 - T)/R$ (where T is the temperature at crystallization time t, R is the cooling rate), the abscissa of temperature in Fig. 4 can be transformed into a time scale. Fig. 5 shows the relative crystallinity as a function of crystallization time. Interestingly, at the same crystallization time, the PET/iPP sample annealed at 200 °C for 5 min has the highest relative crystallinity, followed orderly by neat iPP sample annealed at 200 °C for 5 min, PET/iPP sample annealed at 175 °C for 5 min and neat iPP sample annealed at 175 °C for 5 min. That is, the crystallization of unoriented iPP melt with the presence of PET microfibrils has the highest overall crystallization rate. The most possible explanation has been given as follows: for the neat iPP sample, the ordered clusters in the iPP

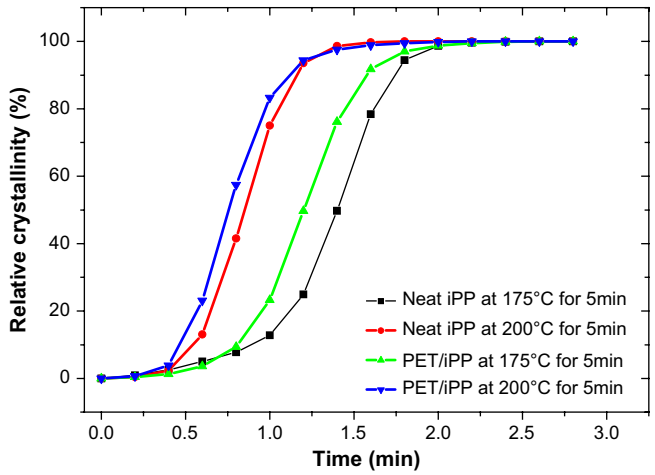

Fig. 5. Plots of relative crystallinity ($X(T)$) vs. crystallization time for neat iPP and PET/iPP microfibrillar blend with different annealing temperatures and annealing time at a predetermined cooling rate of 10 °C/min.

melt can form nuclei at higher crystallization temperature, however, the secondary nucleation as well as growth of lamellae, leading to the increase of crystallinity, has been restrained, therefore, the overall crystallization rate of oriented iPP melt is lower than that of unoriented iPP melt. With the existence of PET microfibrils, the surface of microfibrils can serve as nuclei, this heterogeneous nucleation can take place at higher temperature than common point-like nucleation, which enhances the crystallization rate (see Fig. 5, the curve of PET/iPP at 200 °C for 5 min). Therefore, the overall crystallization rate of oriented iPP melt increases in the presence of PET microfibrils, regardless of unoriented or oriented melt.

3.3. *Crystalline morphology evolution during crystallization of oriented iPP melts*

When the neat iPP sample is annealed at 200 °C for 5 min, the orientation of iPP molecules is hardly preserved due to sufficient relaxation and thus point-like nuclei form at ca. 131 °C, as shown in Fig. 6. As a result, the growth of typical spherulites is observed during nonisothermal crystallization. In contrast, in the oriented iPP melt (annealing at 175 °C for 5 min) (see Fig. 7), the row-nuclei appear at a higher temperature of ca. 150 °C, which are originated from the ordered cluster. And then the fibril-like crystalline morphology as a result of epitaxial crystallization appears at the initial stage of crystallization (see Fig. 7, at 141.2 °C); with the decrease of crystallization temperature, one cannot distinguish between the fibril-like crystalline morphology and the spherulites because of impingement of crystalline fringes (see Fig. 7, at 131.8 °C). One can see that the crystallization temperature range for oriented iPP melt (ca. 150–130 °C), which needs for impingement of adjacent crystalline fringes, is wider than that for the unoriented one (ca. 130–120 °C), indicating strong secondary nucleation at lower crystallization temperature, being in good agreement with the results of DSC. That is, the secondary nucleation other than primary nucleation plays a more important role in overall crystallization rate in the case of neat iPP.

For the PET/iPP microfibrillar sample, when the sample is annealed at 200 °C for 5 min, as shown in Fig. 8, initially, the nucleation almost takes place in the left side of sample where PET microfibrillar network exists, indicating the strong heterogeneous nucleation ability of PET microfibrils. The heterogeneous nucleation leads to the spherulites with smaller size (see Fig. 8, left half region). However, for the oriented sample (annealing at 175 °C for 5 min), the crystallization journey is just the same as the case of oriented neat iPP melt, a distinct fibril-like crystalline morphology was observed firstly and the phenomenon of heterogeneous nucleation was hardly identified in the area of the PET microfibrillar network. The results of DSC and POM indicate that the self-seeded nucleation is dominant in the process of orientation crystallization, which leads to the higher onset crystallization temperature and the formation of fibril-like structure. However, the onset temperature of orientation crystallization can be enhanced further by the striking heterogeneous nucleation with the addition of PET microfibrils (see Fig. 3b), and some sporadic spherulites can be observed in the left side of Fig. 9 (see white arrows), indicating the existence of heterogeneous nucleation. In general, the addition of PET microfibrillar network can accelerate nucleation in oriented iPP

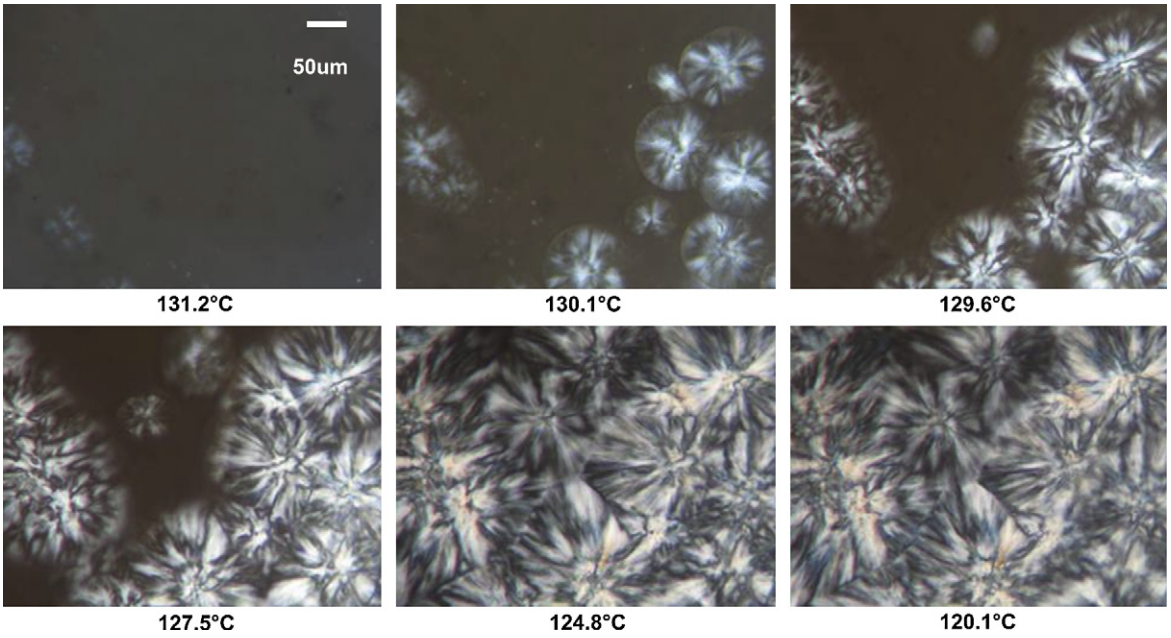

Fig. 6. The evolution of crystalline morphology in unoriented iPP melt, annealing at 200 °C for 5 min with a cooling rate of 2 °C/min.

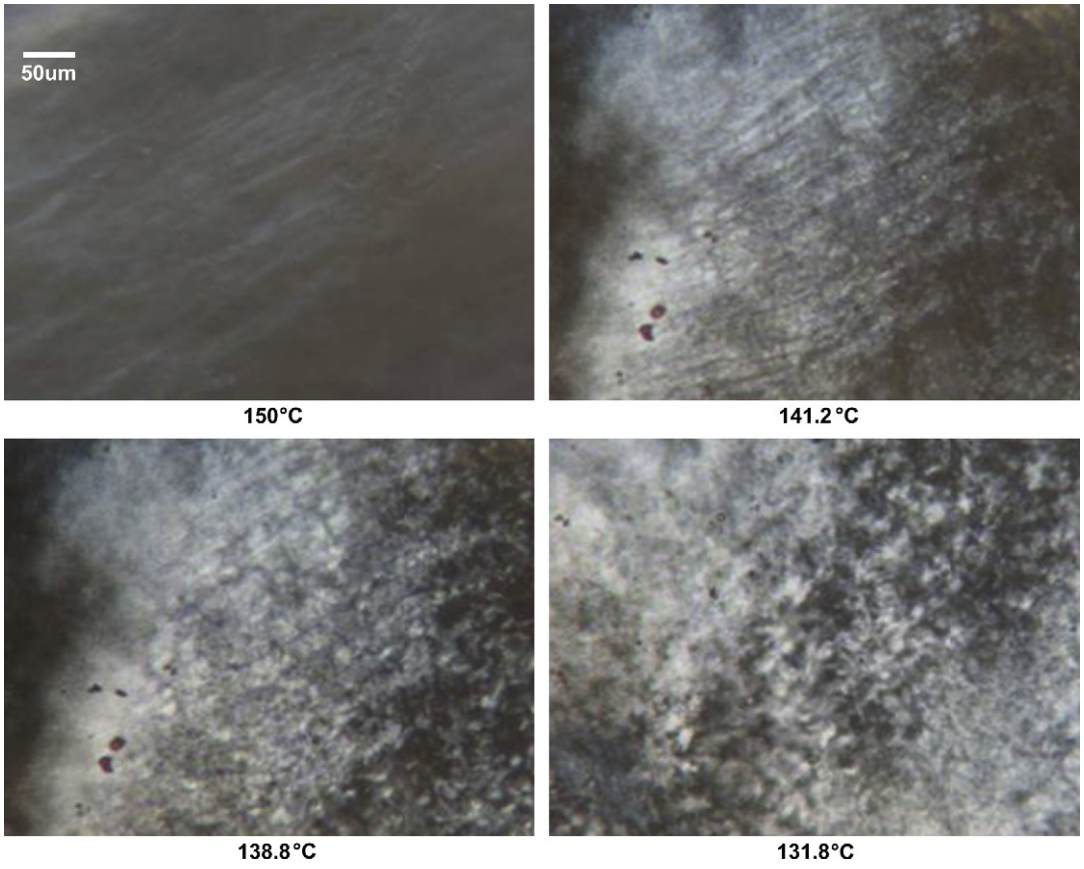

Fig. 7. The evolution of crystalline morphology in oriented iPP melt, annealing at 200 °C for 5 min with a cooling rate of 2 °C/min.

melt, but row nucleation and formation of fibril-like crystalline morphology are dominated in oriented iPP melt.

Furthermore, the length of the fibril-like crystalline morphology formed in the oriented crystallization of iPP melt is in the range between tens of microns and hundreds of microns (see Fig. 7, at 140.1 °C), which is much larger than the length of iPP molecules in the samples ($\overline{M}_n$ is 2.3×10^4 g/mol, the length is several microns). Therefore, it is reasonable to infer that the nucleation of fibril-like structure happened simultaneously in several iPP molecules which are entangled with each other, in which the orientation memory is

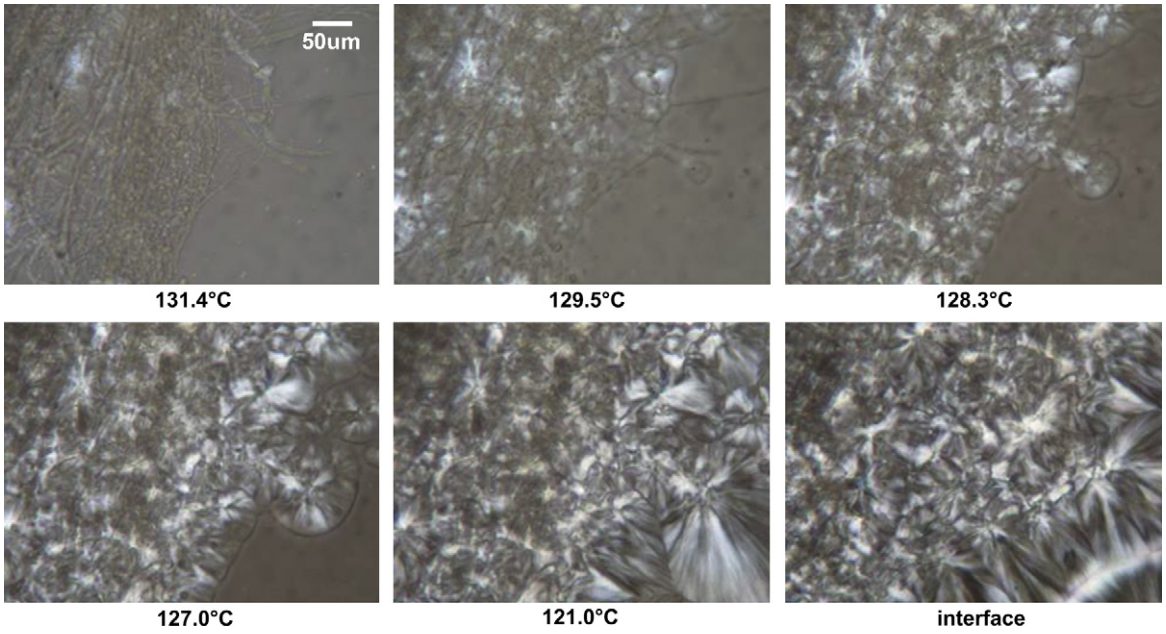

Fig. 8. The crystalline morphology evolution in unoriented iPP melt in the presence of PET microfibrils, annealed at 200 °C for 5 min with a cooling rate of 2 °C/min, the PET microfibrillar network is located at the left side of the pictures.

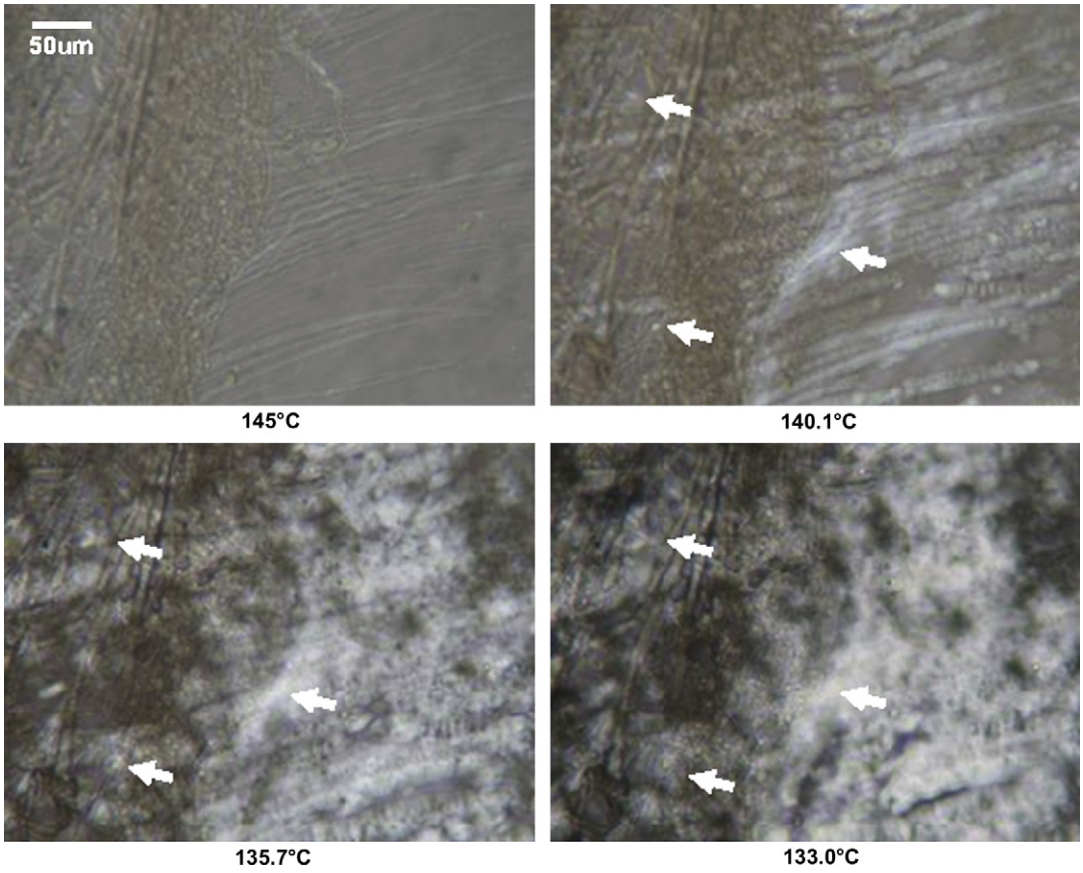

Fig. 9. The crystalline morphology evolution in oriented iPP melt in the presence of PET in situ microfibrils, annealed at 175 °C for 5 min, cooling rate is 2 °C/min, the PET microfibrils are located at left side of the pictures, the white arrows direct the crystalline morphology induced by the heterogeneous nucleation.

preserved as the disentangled chain segments extending between highly entangled knots at lower annealing temperature [35]. Moreover, the similar fibril-like structure was discovered in the process of crystallization of iPP melt under step shear mode of shear hot stage (ca. 0.5 s^{-1}) [36], in which the length is shorter than that in our case, indicating that the stronger shear force can induce the fibril-like structure with longer aspect ratio during SCORIM.

4. Conclusion

The PET/iPP microfibrillar blend was fabricated by "extrusion-hot stretching-quenching" process. The SCORIM technology had been applied for the fabrication of corresponding bars, the shish–kebab structure with higher thermodynamic stability exists in the whole region of the SCORIM samples, especially in skin layers; the existence of PET microfibrillar network seems to homogenize the morphological distribution of shish–kebab structure. Furthermore, the oriented iPP melt was obtained by lower annealing of the skin layer of the bars (i.e. annealed at 175 °C for 5 min), the existence of ordered clusters leads to the primary nucleation at higher onset of crystallization temperature, and the fibril-like crystalline morphology forms in the melt. However, the overall crystallization rate decreases as a result that the relative high crystallization temperature restrained the secondary nucleation as well as lamellae growth. With the existence of PET microfibrils, the heterogeneous nucleation distinctly happens in the unoriented iPP melt and results in the increase of crystallization peak and overall crystallization rate, moreover, for the oriented iPP melt in the presence of PET microfibrils, the onset of crystallization temperature had been accelerated further, indicating the synergistic effect of row nucleation and heterogeneous nucleation.

Acknowledgements

The authors gratefully acknowledge the financial support of this work by National Natural Science Foundation of China (contract no. 50527301) and the open fund of State Key Laboratory of Polymer Materials Engineering (PR China). G. J. Zhong would like to thank Ms. X. Xu for her encouragement.

References

[1] Viana JC. Polymer 2004;45:993–1005.
[2] Mendoza R, Régnier G, Seiler W, Lebrun JL. Polymer 2003;44:3363–73.
[3] Zhu PW, Edward G. Macromol Mater Eng 2003;288:301–11.
[4] Zhu PW, Phillips A, Edward G. J Appl Phys 2005;97:104908.
[5] Fu SY, Lauke B. Compos Sci Technol 1998;58:389–400.
[6] Choy CL, Leung WP, Kowk KW, Lau FP. Polym Compos 1992;13:69–80.
[7] Zhu PW, Tung J, Phillips A, Edward G. Macromolecules 2006;39:1821–31.
[8] Zhu PW, Edward G. Polymer 2004;45:2603–13.
[9] Dikovsky D, Marom G, Avila-Orta CA, Somani RH, Hsiao BS. Polymer 2005;46:3096–104.
[10] Larin B, Marom G, Avila-Orta CA, Somani RH, Hsiao BS. J Appl Polym Sci 2005;98:1113–8.
[11] Larin B, Avila-Orta CA, Somani RH, Hsiao BS, Marom G. Polymer 2008;49:295–302.
[12] Tadmor Z. J Appl Polym Sci 1974;18:1753–72.
[13] Kumaraswamy G. J Macromol Sci Part C Polym Rev 2005;45:375–97.
[14] Kumaraswamy G, Issaian AM, Kornfield JA. Macromolecules 1999;32:7537–47.
[15] Kumaraswamy G, Verma RK, Issaian AM, Wang P, Kornfield JA, Yeh F, et al. Polymer 2000;41:8931–40.
[16] Azzurri F, Alfonso GC. Macromolecules 2005;38:1723–8.
[17] Somani RH, Yang L, Hsiao BS. Physica A 2002;304:145–57.
[18] Somani RH, Yang L, Zhu L, Hsiao BS. Polymer 2005;46:8587–623.
[19] Kimata S, Sakurai T, Nozue Y, Kasahara T, Yamaguchi N, Karino T, et al. Science 2008;316:1014–7.
[20] Na B, Wang Y, Zhang Q, Fu Q. Polymer 2004;45:6245–60.
[21] Li ZM, Yang MB, Xie BH, Feng JM, Huang R. Polym Eng Sci 2003;43:615–28.

[22] Li ZM, Yang W, Xie BH, Huang R, Yang MB. Macromol Mater Eng 2004;289:349–54.
[23] Li ZM, Yang W, Li LB, Xie BH, Huang R, Yang MB. J Polym Sci Part B Polym Phys 2004;42:374–85.
[24] Li ZM, Li LB, Shen KZ, Yang MB, Huang R. J Polym Sci Part B Polym Phys 2004;42:4095–106.
[25] Li ZM, Li LB, Shen KZ, Yang W, Huang R, Yang MB. Macromol Rapid Commun 2004;25:553–8.
[26] Kalay G, Zhong ZP, Allan P, Bevis MJ. Polymer 1996;37:2077–85.
[27] Guan Q, Shen KZ, Ji JL, Zhu JM. J Appl Polym Sci 1995;55:1797–804.
[28] Zhong GJ, Li ZM, Li LB, Mendes E. Polymer 2007;48:1729–40.
[29] Zhong GJ, Li LB, Mendes E, Byelov D, Fu Q, Li ZM. Macromolecules 2006;39:6771–5.
[30] Mano JF, Sousa RA, Reis RL, Cunha AM, Bevis MJ. Polymer 2001;42:6187–98.
[31] Li ZM, Yang MB, Feng JM, Huang R. Mater Lett 2002;56:756–62.
[32] Fujiyama M, Wakino T. J Appl Polym Sci 1988;35:29–49.
[33] Li ZM, Li LB, Shen KZ, Yang MB, Huang R. Polymer 2005;46:5358–67.
[34] Cho K, Kim D, Yoon S. Macromolecules 2003;36:7652–60.
[35] Stribeck N, Almendarez CA, Bayer R. Macromol Chem Phys 2004;205:1463–70.
[36] Zhang CG, Hu HQ, Wang DJ, Yan SK, Han CC. Polymer 2005;46:8157–61.